

Journal Pre-proof

Cloud Scattering Impact on Thermal Radiative Transfer and Global Longwave Radiation

Zhonghai Jin , Yuanchong Zhang , Anthony Del Genio ,
Gavin Schmidt , Maxwell Kelley

PII: S0022-4073(19)30508-4
DOI: <https://doi.org/10.1016/j.jqsrt.2019.106669>
Reference: JQSRT 106669



To appear in: *Journal of Quantitative Spectroscopy & Radiative Transfer*

Received date: 19 July 2019
Revised date: 20 September 2019
Accepted date: 21 September 2019

Please cite this article as: Zhonghai Jin , Yuanchong Zhang , Anthony Del Genio , Gavin Schmidt , Maxwell Kelley , Cloud Scattering Impact on Thermal Radiative Transfer and Global Longwave Radiation, *Journal of Quantitative Spectroscopy & Radiative Transfer* (2019), doi: <https://doi.org/10.1016/j.jqsrt.2019.106669>

This is a PDF file of an article that has undergone enhancements after acceptance, such as the addition of a cover page and metadata, and formatting for readability, but it is not yet the definitive version of record. This version will undergo additional copyediting, typesetting and review before it is published in its final form, but we are providing this version to give early visibility of the article. Please note that, during the production process, errors may be discovered which could affect the content, and all legal disclaimers that apply to the journal pertain.

© 2019 Published by Elsevier Ltd.

Highlights:

- LW cloud scattering effect on radiation fluxes and its spectral variation and dependence on cloud properties are investigated.
- An efficient radiative transfer scheme to explicitly consider the LW scattering is implemented to the GISS GCM for accurate calculation of radiation.
- LW cloud scattering effect is nonnegligible in climate modeling.

Journal Pre-proof

Cloud Scattering Impact on Thermal Radiative Transfer and Global Longwave Radiation

Zhonghai Jin¹, Yuanchong Zhang^{1,2}, Anthony Del Genio¹, Gavin Schmidt¹,
Maxwell Kelley^{1,2}

¹NASA Goddard Institute for Space Studies, New York, NY 10025

²SciSpace, LLC, New York, NY, USA

Corresponding author address:

Zhonghai Jin

NASA Goddard Institute for Space Studies

2880 Broadway, New York, NY 10025

email: Zhonghai.jin@nasa.gov

Abstract

The potential importance of longwave (LW) cloud scattering has been recognized but the actual estimate of this effect on thermal radiation varies greatly among different studies. General circulation models (GCMs) generally neglect or simplify the multiple scattering in the LW. In this study, we use a rigorous radiative transfer algorithm to explicitly consider LW multiple-scattering and apply the GCM to quantify the impact of cloud LW scattering on thermal radiation fluxes. Our study shows that the cloud scattering effect on downward thermal radiation at the surface is concentrated in the infrared atmospheric window spectrum (800–1250 cm^{-1}). The scattering effect on the outgoing longwave radiation (OLR) is also present in the window region over low clouds but it is mainly in the far-infrared spectrum (300–600 cm^{-1}) over high clouds. For clouds with small to moderate optical depth ($\tau < 10$), the scattering effect on thermal fluxes shows large variation with the cloud τ and has a maximum at an optical depth of ~ 3 . For opaque clouds, the scattering effect approaches an asymptote and is smaller and less important.

The 2-stream radiative transfer scheme could have an error over 10% with an RMS error around 3.5%-4.0% in the calculated LW flux. This algorithm error of the 2-stream approximation could readily exceed the no-scattering error in the LW, and thus it is worthless to include the time-consuming computation of multiple scattering in a 2-stream radiative transfer scheme. However, the calculation error rapidly decreases as stream number increases and the RMS error in LW flux using the 4-stream scheme is under 0.3%, an accuracy sufficient for most climate studies. We implement the 4-stream discrete-ordinate algorithm in the GISS GCM and run the GCM for 20 years with and without the LW scattering effect, respectively. When cloud LW scattering is included, we find that the global annual mean OLR is reduced by 2.7 W/m^2 , and the downward surface flux and the net atmospheric absorption are increased by 1.6 W/m^2 and 1.8

W/m^2 , respectively. Using one year of ISCCP clouds and running the standalone radiative transfer offline, the global annual mean non-scattering errors in OLR, surface LW downward flux and net atmospheric absorption are 3.6 W/m^2 , -1.1 W/m^2 , and -2.5 W/m^2 , respectively. The global scattering impact of 2.7 W/m^2 on the OLR is small when compared to the typical global OLR value of 240 W/m^2 , but it is significant when compared to cloud LW radiative forcing (30 W/m^2) and net cloud forcing (-14 W/m^2). Overall, the effect of neglecting scattering on the thermal fluxes is comparable to the reported clear sky radiative effect of doubling CO_2 .

Keywords: longwave cloud scattering, radiative transfer, longwave radiation

1. Introduction

The law of conservation of energy requires that in equilibrium, the energy absorbed by the Earth from the sun balance the energy radiated by the Earth back into space. This balance in radiation energy drives the Earth's climate. The radiation budget of the Earth-atmosphere system is long studied. While clouds, aerosols and various atmospheric gases all affect the radiation energy by absorption and scattering, the clouds have the most significant impact on Earth's radiation budget. Clouds cover about three-quarters of the planet according to observations made by the CloudSat and CALIPSO satellites (Mace et al., 2014) and small changes in cloud cover have a large impact on the climate (Cess et al., 1990). Clouds both reflect incoming sunlight and inhibit infrared radiation emitted by the surface and the lower troposphere, thereby affecting both sides of the global energy balance equation.

Climate studies often simplify the longwave (LW) radiative transfer by directly neglecting the cloud scattering or simply applying an ad-hoc correction to account for it. These simplifications are assumed because 1) LW radiative transfer in clouds is dominated by the absorption of water vapor and water/ice particles and the effect of scattering is relatively weak; 2) Multiple scattering calculations in atmospheric radiative transfer require a great amount of computing time, especially when there are multiple partly cloudy layers. However, a number of studies show that the cloud LW scattering could have a nonnegligible impact on Earth's radiation energy budget (Chou, 1999; Stephens et al., 2001; Costa and Shine, 2006; Kuo et al., 2017; Tang et al., 2018; Zhao et al., 2018; Wu et al., 2019). Although all these studies agree that ignoring the cloud LW scattering would overestimate the Outgoing LW Radiation (OLR) and underestimate the downwelling thermal radiation at the surface, the estimated amount of this scattering effect varies over a wide range. For example, when scattering by clouds is included, Stephens et al. (2001) estimated that the global mean OLR decreases by 8 W/m^2 , Costa and Shine (2006) showed a global OLR reduction of approximately 3 W/m^2 , and Schmidt et al. (2006) stated that OLR decreases by approximately 1.5 W/m^2 and surface downward flux increases by about 0.4 W/m^2 . Using satellite observational data, Kuo et al. (2017) showed that neglecting cloud scattering could result in an overestimation of the global mean OLR of 2.6 W/m^2 and an underestimation of the downwelling LW radiation at the surface of 1.2 W/m^2 . The large variety in the estimated cloud LW scattering impact among different studies could be attributed to the different data and different algorithms used for the calculation. For example, an approach by adjusting the atmospheric and cloud optical properties was used to account for the LW scattering in the Goddard Institute for Space Studies (GISS) ModelE General Circulation Model (GCM) by Schmidt et al. (2006) and in the Goddard Earth Observing System GCM by Chou (1999), a

perturbation method (Li, 2002) was used by Wu et al. (2019), and a two-stream radiative transfer approximation was used by Stephens et al. (2001). The large number of 8 W/m^2 of OLR difference in Stephens et al. (2001) is possibly due to the error in the two-stream scheme, which is easily of the order of few W/m^2 in the OLR as to be presented in this study. A more accurate multi-stream discrete-ordinate algorithm was used in the studies by Costa and Shine (2006) and by Kuo et al. (2017), but cloud information was from limited climatological or observational data.

In this study, we use the discrete-ordinate algorithm to explicitly include the cloud scattering in the LW flux calculations. In order to evaluate the cloud LW scattering effect in a climate modeling environment, the algorithm is implemented in the GISS global climate model (ModelE2.1) and the model is then run with and without the cloud scattering included, respectively. In this paper, the methodology for calculating multiple scattering by clouds in the thermal radiative transfer is described in section 2. The sensitivity study on different cloud property effects on LW scattering is presented in section 3 and the global estimates from both the GCM simulation and the offline radiative transfer computation are presented in section 4. Finally, conclusions are given in section 5.

2. LW radiative transfer

Since only the flux calculations are concerned in this study, we introduce the azimuthally averaged LW radiative transfer equation. When multiple scattering is considered, this equation for a plane-parallel atmosphere with local thermodynamic equilibrium can be written as

$$\mu \frac{dI(\tau, \mu)}{d\tau} = I(\tau, \mu) - \frac{\omega(\tau)}{2} \int_{-1}^1 I(\tau, \mu') P(\tau, \mu, \mu') d\mu' - (1 - \omega(\tau)) B(T), \quad (1)$$

where I is the diffuse thermal radiance, τ the normal optical depth, and ω the single scattering albedo. μ and μ' represent the cosines of the angles between the propagating direction of I and

the zenith and $P(\tau, \mu, \mu')$ is the azimuthally averaged scattering phase function. $B[T(\tau)]$ is the blackbody radiance (Planck function) at temperature T . The wavelength dependence of all quantities is omitted in Equation (1) for simplicity. The second term on the right hand side of Equation (1) represents the multiple scattering source. When the scattering effect is neglected, the radiative transfer equation can be simplified to the form

$$\mu \frac{dI(\tau, \mu)}{d\tau} = (1 - \omega(\tau))I(\tau, \mu) - (1 - \omega(\tau))B(T). \quad (2)$$

Equation (2) can be derived from Equation (1) by assuming the scattering phase function P as the δ function. This is equivalent to assuming that all scattering occurs in the original direction of propagation only, that is total forward scattering. Because the absorption optical depth $\tau_a = \tau(1 - \omega)$, Equation (2) can be rewritten as

$$\mu \frac{dI(\tau, \mu)}{d\tau_a} = I(\tau, \mu) - B(T). \quad (3)$$

When $\omega = 0$ (no scattering), Equation (1) becomes the same as Equation (3) except that τ is replaced by τ_a . This indicates that the best treatment of non-scattering cloud properties in radiative transfer is by setting the scattering optical depth to zero so that the extinction is described by absorption only, rather than simply by ignoring the scattering term (the second term) on the right hand side of Equation (1).

For a non-isothermal layer, the optical depth dependence of the Planck function $B[T(\tau)]$ is needed to solve the radiative transfer equation. Following Fu et al. (1997), an exponential optical depth dependence for the Planck function can be used, which is expressed as

$$B[T(\tau)] = B_0 e^{\beta\tau} \quad (4)$$

Where $\beta = (1/\tau_1) \ln(B_1/B_0)$, τ_1 is the layer optical depth, and B_0 and B_1 represent the Planck functions at the top and the bottom of the layer, respectively. A variety of techniques have been

developed to solve the radiative transfer equation. When the scattering is neglected, the upward and downward radiances are independent of each other and an analytical solution can be achieved (Fu et al., 1997, Li and Fu, 2000). The exit radiances at the layer boundaries for this particular case can be derived as

$$I(0, +\mu) = I(\tau_1, +\mu)e^{-\tau_a/\mu} + \frac{1-\omega}{\mu\beta-1+\omega} (B_1e^{-\tau_a/\mu} - B_0) \quad (5a)$$

$$I(\tau_1, -\mu) = I(0, -\mu)e^{-\tau_a/\mu} + \frac{1-\omega}{\mu\beta+1-\omega} (B_0e^{-\tau_a/\mu} - B_1) \quad (5b)$$

Where $\tau_a = \tau_1(1 - \omega)$ is the absorption optical depth.

When the scattering is considered, however, the upward and downward radiances are coupled through the scattering function and there exists no simple analytical solution as Equation (5), unless a simple numerical scheme like the two-stream or four-stream approximation is used. A 2-stream approximation and the similar Edington approach assume the scattering phase function as a simple two term function, and therefore the analytical solution can be achieved (e.g., Chandrasekhar, 1960; Meador and Weaver, 1980; Liou, 2002). After a lengthy derivation, Liou et al. (1988) obtained an analytical four-stream solution of radiative transfer with multiple scattering. Using the two-stream source function, Fu et al. (1997) further developed a simplified four-stream analytical solution specifically for the LW radiative transfer with scattering included. The detailed derivation is referred to Fu et al. (1997) and here only the solution for this special four-stream case is presented:

$$I(0, +\mu) = I(\tau_1, +\mu)e^{-\tau_1/\mu} + \frac{c_1(1-k/D)}{\pi(k\mu-1)} (e^{-\tau_1/\mu} - e^{k\tau_1}) + \frac{c_2R(1+k/D)}{\pi(k\mu+1)} (1 - e^{\tau_1(k+1/\mu)}) + \frac{\epsilon}{1-\mu\beta} (B_0 - B_1e^{-\tau_1/\mu}) \quad (6a)$$

$$I(\tau_1, -\mu) = I(0, -\mu)e^{-\tau_1/\mu} + \frac{c_2(1-k/D)}{\pi(k\mu-1)} (e^{-\tau_1/\mu} - e^{k\tau_1}) + \frac{c_1R(1+k/D)}{\pi(k\mu+1)} (1 - e^{\tau_1(k+1/\mu)}) + \frac{\eta}{1+\mu\beta} (B_1 - B_0e^{-\tau_1/\mu}) \quad (6b)$$

Where k, R, ϵ and η all are a function of the single scattering albedo ω and the scattering asymmetry factor g . C_1, C_2 and D are constants. μ here is positive from the double Gauss quadrature.

In general, given the solution for the upward and downward radiances, the upwelling (F_u) and downwelling (F_d) fluxes can be obtained as following (Stamnes et al., 1988; Liou, 2002):

$$F_u(0) = 2\pi \int_0^1 \mu I(0, +\mu) d\mu = 2\pi \sum_{i=1}^n w_i \mu_i I(0, +\mu_i) \quad (7a)$$

$$F_d(\tau_1) = 2\pi \int_0^1 \mu I(\tau_1, -\mu) d\mu = 2\pi \sum_{i=1}^n w_i \mu_i I(\tau_1, -\mu_i) \quad (7b)$$

Where n is the number of quadrature angles used for radiance computation and flux summation, and w_i is the weight associated with the radiance at the i th direction. $N=2n$ is the so-called stream number for the radiative transfer solution. While the computation accuracy increases with the stream number, the computation time also grows at a great rate (roughly as the cube of the stream number). Because of its computation efficiency, a two-stream approximation or a similar scheme is commonly adopted in the GCM models. For calculation of the thermal infrared flux, however, the algorithm error introduced by the two-stream approximation itself, even with multiple scattering considered, could be larger than that introduced by neglecting the scattering effect in an accurate higher order stream calculation (Fu et al., 1997). Therefore, a compromise between computational accuracy and speed must be made for climate modeling.

For an illustration, Figure 1 shows how the computation accuracy in LW radiation varies with the stream number. For simplicity, an isothermal layer of cloud is used here and only the internal thermal radiation source is included, but the multiple scattering is explicitly considered. Under these assumptions, the exit fluxes at the upper and lower boundaries are the same and only one is plotted in Figure 1. For each stream number, there are a total of 200 calculations, representing 200 different cloud optical depths. The optical depths are selected randomly

between 0.5 and 20.0 and then each optical depth is used to calculate the flux using different number of streams. The LW flux reaches the asymptotic value near optical depth of 20 and thus there is no need to consider optical depth beyond 20. As the stream number increases, the calculated flux quickly converges to the exact solution. The converged 24-stream LW flux is used as the benchmark and then the fluxes calculated using other stream numbers are normalized by the benchmark value. Therefore, any divergence from the 1.0 in this normalized or relative flux represents the computational error. For example, a relative flux of 1.05 in Figure 1 indicates an error of 5%. Listed in Figure 1, the number below the flux distribution plot for each stream number represents the relative RMS error (%) for the group of fluxes (total of 200) calculated using that stream number. For ice cloud optical properties, we use the surface-roughened aggregate model used in the MODIS Collection 6 (C6) satellite cloud retrieval product (Platnick et al., 2017). For liquid cloud, the spherical water particle model developed by Hu and Stamnes (1993) is used. The effective radii of 40 μm and 10 μm are assumed for the ice and water clouds, respectively. However, neither the normalized flux distribution nor the RMS error shows considerable variation with the cloud particle size (not shown).

The tests in Figure 1 are for a single cloud layer with absorption and scattering by cloud particles only. When it is placed into an actual atmosphere, the LW flux error would become smaller because of the additional atmospheric absorption and the flux contribution from the assumed isotropic surface thermal emission. Figure 1 shows that the 2-stream scheme could have an error over 10% in LW flux. Using the Delta-Eddington approach, a scheme similar to the 2-stream approximation, the computation accuracy would not be improved but little worse (not shown). The RMS error of the 2-stream approximation is approximately 3.7%, that is indeed larger than the effect of neglecting the LW cloud scattering to be studied (about 1%). This

justifies the no-scattering approximation adopted in the climate models which use a 2-stream radiative transfer scheme. However, the results in Figure 1 rapidly converge as the stream number increases. The RMS error of the 4-stream scheme is under 0.3%, which is sufficient for the accuracy requirement in most climate studies.

3. Cloud scattering effect on LW radiation

Using the radiative transfer solutions with and without scattering considered, we first conduct some sensitivity tests to understand how the LW scattering impact varies with cloud optical and physical properties. The ice and water cloud models described in section 2 are also used here. These cloud optical properties are implemented in our coupled ocean-atmosphere radiative transfer (COART) model (Jin et al., 2006) and this model is used for the radiative transfer calculation here. COART can conveniently be reduced to the conventional radiative transfer model for the atmosphere-surface system when desired. The discrete ordinate method (DOM) is used to solve the radiative transfer equation and the stream number is flexible to choose in COART input. The atmospheric absorption database is adopted from the MODTRAN code and has different spectral resolutions available up to 0.1 cm^{-1} (Berk et al., 2008).

The left panels in Figure 2a show the COART model simulated spectral upward flux at the top of the atmosphere (TOA) and the downward flux at the surface, respectively. In each panel, the black line represents the computation with cloud scattering included and the red line represents the computation without cloud scattering. As an example, fluxes are calculated for the standard midlatitude summer atmosphere using the 16-stream DOM and with spectral resolution of 5 cm^{-1} . Results are shown for a high cloud with ice particle effective radius (R_e) of $40 \text{ }\mu\text{m}$, top height of 11 km and thickness of 1 km. The cloud optical depth is 10 in the visible (550 nm) and it varies with wavelength. The right two panels show the corresponding spectral difference

between the two computations (without scattering – with scattering), representing the flux error of neglecting scattering. The spectrally integrated LW fluxes and flux differences are presented in the upper-right corner in each panel. Figure 2b is the same as 2a except for a low water cloud ($R_e=10\ \mu\text{m}$, top height of 4 km). Results in Figure 2a and 2b show that the no-scattering flux error at the surface is concentrated in the infrared atmospheric window region (about 800–1250 cm^{-1}) and this is also true for the upward flux at TOA over the low cloud. However, the effect of neglecting cloud scattering for the OLR over the high cloud is mainly in the far-infrared spectral region (around 300–600 cm^{-1}) as shown in the upper-right panel in Figure (2a). This results from the reduced absorption due to the lower water vapor amount over a high cloud.

For the same high and low clouds and same atmospheric model defined above, Figure 3 shows the same no-scattering error in the total downward LW radiation at the surface (the dashed lines) and the OLR (the solid lines) as a function of the cloud visible optical depth. The results show that error in the OLR is always larger than that in the downward radiation at the surface and all errors reach a maximum at cloud optical depth of about 3. Fixing the cloud optical depth at 3.0, Figure 4 shows the same no-scattering flux errors versus the cloud particle effective radius. All the flux errors of neglecting scattering increase as the cloud particle size decreases, particularly for clouds with small particle sizes which have higher scattering efficiency.

4. Global effect of the LW cloud scattering

We have demonstrated how the LW flux error from neglecting cloud scattering varies with different cloud properties in section 3. While the 16-stream algorithm used for these sensitivity tests is computationally too expensive to quantify this LW scattering effect globally in climate modeling, the 2-stream approximation scheme or its equivalent is too erroneous to correctly account for the multiple scattering effect. The special 4-stream solution introduced in

section 2 is not only computationally efficient but also sufficiently accurate, and therefore it is a good choice to be used to calculate the LW radiation over large time and space scales.

In order to evaluate the cloud LW scattering impact on climate modeling exactly, we implement the special 4-stream radiative transfer algorithm into the GISS climate model (ModelE2.1) (Schmidt et al., 2014). LW calculations in ModelE use the correlated k distribution with 33 intervals (Lacis and Oinas 1991; Oinas et al. 2001), designed to match line-by-line computed fluxes and cooling rates throughout the atmosphere to within about 1%. The thermal fluxes in ModelE were calculated using a no-scattering format with parameterized correction factors applied to the outgoing TOA flux to account for multiple scattering effects using tabulated data from offline calculations. The newly implemented radiative transfer scheme enables ModelE to explicitly include the LW scattering process. In addition, several new cloud parameterizations of optical properties (Platnick, 2017; Baum, 2014), including that for the MODIS C6 cloud model, are implemented into ModelE. These new cloud optics models include different ice particulate habits. The old ice cloud optics model in ModelE severely suppress the LW scattering because (1) the spherical or spheroid particle shape is used, which backscatters less LW radiation than hexagonal crystals, and (2) it is based on the old compilation of the spectral absorption coefficient of ice, which has significant larger absorption than the updated compilation in LW spectrum (Warren and Brandt, 2008).

The ModelE uses a 30-min time step for all physics calculations. The radiation code is called every five physics time steps (every 2.5 h). Using the present day climate with the prescribed sea surface temperature (SST), we run ModelE twice for 20 years (1980-2000) to eliminate the weather noise and the only difference between the two runs is the cloud LW scattering. To isolate the LW scattering effect, the original LW scattering correction in ModelE

is shut off in both the model runs. Figure 5 shows the 20-year averaged LW radiation differences between the two calculations (without scattering – with scattering), representing the cloud scattering effect on the thermal radiation in the climate model. Large LW scattering effects on the OLR (upper panel) and atmospheric absorption (lower panel) can be found along the Intertropical Convergence Zone (ITCZ) with maximum OLR bias of 8.5 W/m^2 . Large scattering effects on the downward surface flux (middle panel) are seen in the polar and high-altitude regions because more scattered LW flux can reach the surface due to smaller atmospheric absorption under the clouds. The global mean no-scattering error in the OLR is 2.7 W/m^2 and the error in the downward flux at the surface is 1.6 W/m^2 . While the 20-year average is presented here, the 10-year average gives very similar results, for example, the average errors over 1980 to 1989 are 2.7 W/m^2 and 1.5 W/m^2 in the upward and downward LW fluxes, respectively. Moreover, the spatial patterns for the two time frames are also very similar. These indicate that the model internal variability has little effect on the results averaged over the 20-year time frame.

The optics model of MODIS C6 cloud we adopted assumes an ensemble of aggregates composed of eight severely roughened columns for ice cloud particles. To test the possible effect of ice particulate habit, we run the GISS ModelE as for Figure 5 but using the ice cloud optical properties for the particle shape of solid column (Baum et al., 2014). The results turn out to be very similar to that from using the aggregate habit.

There exist complex interactions among components of the Earth system. In response to the LW radiation change resulting from the LW cloud scattering, a number of climate variables could change, including the atmospheric temperature and water vapor amount. These changes will in turn change the atmospheric dynamics and thermodynamics and the cloud properties. Figure 6 shows the 20-year averaged differences in cloudiness (in percentage) corresponding to

the LW radiation changes shown in Figure 5. The upper, middle and lower panels represent the high, the low and the total cloudiness, respectively. The spatial pattern of the high cloud change is similar to that of the total cloud, indicating that high cloud dominates the total cloud change. While the cloud response may have a significant contribution to the LW radiation change locally, the global average of this effect might be small because the global mean cloudiness change is only about 0.1% and the ratio of this cloudiness change to the interannual variability (standard deviation of cloudiness) across the 20 years is only 0.15. Same as the radiation changes, the magnitude and spatial pattern of the cloudiness difference in the first 10-year average are similar to the 20-year mean shown in Figure 6, confirmed the small effect of model internal variability on an average over a time frame longer than 10 years.

Among the various cloud properties, the change in cloud fraction is mainly responsible for the LW radiation changes presented, because no significant correlation is found between the radiation change and other cloud property changes such as optical depth and particle size. Figure 7 shows the scattering affected changes in cloud fraction and LW radiation (with – without scattering) and their correlations. All changes are in global annual mean, calculated for each of the twenty years. The black line in each panel represents a different radiation change (in W/m^2) across the twenty years, with the upper panel for the OLR, the middle panel for the downward surface flux and the lower panel for the atmospheric absorption. The three colored lines in each panel represent the changes in the high, low and total cloudiness (%), respectively. For a better display, the cloudiness changes in each panel are offset by the 20-year mean of the respective radiation change. The correlation coefficients between the change in radiation and the changes in cloud amount are listed in the lower right corner of each panel. The results show that the change in the OLR has a high anticorrelation (-0.764) with the change in the total cloudiness, while the

atmospheric absorption is positively correlated (0.632) with the total cloudiness. The correlation between the surface flux change and the cloud amount change is low (the middle panel). For each radiation change, its correlation with high cloud is much higher than that with low cloud and there is no significant correlation with the low cloud change, indicating that the LW radiation change due to the LW scattering effect and the associated cloud response are dominated by high clouds.

For this GCM simulation, we have also calculated the profile of the thermal radiation cooling rate for both the model runs. Figure 8 shows the 20-year averaged difference in the zonal mean cross section of the cooling rate (without scattering minus with scattering). The vertical variation of the cooling rate change is obvious. Neglect of the cloud LW scattering increases the cooling rate in the troposphere but decreases it near the tropopause, consistent with the flux changes shown in Figure 5.

In order to estimate the no-scattering errors in a more realistic, physical world, we calculate the same LW radiation globally (without and with LW scattering) as the GCM computation above, using the atmospheric and cloud properties from the International Satellite Cloud Climatology Project (ISCCP) H-series product, which is the latest third-generation product (Young et al, 2018). Besides the retrieved atmospheric and surface properties, the ISCCP H-series product supplies 18-type clouds with the information of cloud amount, column optical thickness, phase information (liquid or ice), cloud height and temperature for each type of cloud. ISCCP-H uses 10-km-sampled B1 (Instead of every-30-km-sampled B3 used for ISCCP-D) for its production. There are also other refinements in radiance quality control, calibration, cloud detection (especially high, thin and polar clouds), and cloud and surface property retrievals with improved ancillary datasets (e.g., more accurate surface type and topography, snow/ice datasets,

reprocessed ozone data). The temperature and humidity profiles with increased vertical resolution have been statistically adjusted to have diurnal variation wherever suitable. The new ISCCP H-series has also increased sub-data product categories (e.g., five for L3) at 110-km resolution with a new globally gridded pixel-level (L2) data at 10-km resolution. For more detailed information, it is referred to Young et al. (2018).

The ISCCP-FH production code, which is used to produce the radiative flux profile using the ISCCP H-series product, is used for the radiative transfer computation (Zhang et al., 2019). The original ISCCP-FH production code is basically the standalone radiative transfer code of the GISS ModelE2 with a number of improvements. To be consistent with the GCM computation, the aforementioned 4-stream scheme and the MODIS C6 cloud model are also implemented in the ISCCP-FH production code. The Vertical Cloud Layer Configuration (VCLC) algorithm is used that consists of two parts: (1) cloud vertical structure (CVS) model-B (Zhang et al., 2004), and (2) Cloud Layer Thickness Configuration (CLTC) algorithm based on a combination of 20-year rawinsonde and 5-year CloudSat-CALIPSO climatology. The particle sizes of both the liquid and ice clouds are specified using the climatological monthly mean effective radius retrieved from ISCCP-DX data by Han et al. [1994, 1999].

We have completed 3-yr tests for 1993, 1994 and 1995 based on 3-hourly flux calculations on an equal area map of 110-km resolution. The year 1993 is a normal year without El Nino or La Nina while 1994 and 1995 are ‘moderate’ El Nino and La Nina years, respectively. Their results are very similar, and their global, annual means are very close with the OLR biases of 3.58 W/m^2 , 3.71 W/m^2 , and 3.48 W/m^2 , and the downward surface flux biases of -1.08 W/m^2 , -1.09 W/m^2 , and -1.01 W/m^2 for the three years, respectively. Therefore, we only show the 1993 results here. Figure 9 shows the counterpart of Figure 5, but for the error

estimates of 1993 annual mean LW fluxes based on the ISCCP product. Although it shows the same global parameters as Figure 5, they have quite different meanings. Figure 9 is based on observed atmospheric (including clouds) and surface properties without any feedbacks involved, while Figure 5 is based on 20-yr GCM running that involves a number of feedbacks or interactions among all the possible components in GCM model over the time. Similar to the GCM results, Figure 9a also shows striking overestimates (up to 9 W/m^2 or so) in OLR along the ITCZ, the South Pacific Convergence Zone (SPCZ) and the 60° S band as well as other areas such as the Tibetan Plateau and the North Atlantic Ocean areas. All these areas have a relatively high amount of ice clouds (e.g., King et al., 2013) that contribute large errors due to neglect of LW scattering. The underestimate for downward LW fluxes is relatively small since it is mainly determined by low clouds (Figure 9b). The negative bias of atmospheric absorption of LW flux in Figure 9c is somehow compensation to the positive bias of OLR.

Similar to Figure 8, Figure 10 shows the effect of LW scattering on the thermal radiation cooling rate derived from the ISCCP 1993 data. Same as that from the ModelE simulation, the cooling rate is also increased in the troposphere when the cloud LW scattering is neglected. There is a large difference in the cooling rate profile between the GCM and ISCCP simulations in the polar regions. This difference is caused by the different clouds used by ModelE and ISCCP. ISCCP clouds are more in error over the polar regions than anywhere else (Rossow and Zhang, 2010).

Figure 11 shows the annual zonal mean biases in LW radiation due to the neglect of LW cloud scattering. The upper panel represents the 20-year average from the GISS ModelE and the lower panel represents the annual mean derived from a year (1993) of ISCCP data. The GCM and ISCCP results show similar latitude variation of LW scattering effect but differ significantly

in the polar regions. For example, larger biases for the downward surface flux and lower biases for the OLR and atmospheric absorption are shown in the polar regions in the GCM results, but they are not shown in the ISCCP simulations. This difference is, again, due to the significant difference in clouds between the two.

The global and annual mean no-scattering errors in thermal radiation from different simulations above are summarized in Table 1. Spherical particle shape is assumed for water clouds in all studies listed in the table and the aggregate habit is assumed for ice clouds except for the second GCM run. As shown in Table 1, these errors would not change much when the cloud ice particle shape is changed from aggregate to solid column. The relevant results from Kuo et al. (2017) (hereafter referred to as Kuo2017), which used the same MODIS C6 cloud optics as used here, are also listed in the table for comparison. They obtained the no-scattering error of 2.6 W/m^2 in OLR at the TOA and of 1.2 W/m^2 in downward flux at the surface, respectively, very close to our GCM estimation. The calculation in Kuo2017 is based on one year of satellite observational data, including MODIS retrieved cloud optical thickness and microphysical properties. Different from the GCM results, the radiation biases from the ISCCP simulation and from Kuo2017 represent the transient change because the radiation feedback is not involved. The relatively large differences between the ISCCP and Kuo2017 in Table 1 can be explained by the very different cloud datasets used between the two studies. For example, Kuo2017 uses single-layer clouds but with cloud top and base heights defined by CALIPSO and CloudSat, while ISCCP uses multi-layer clouds with 18 types. Cloud height and vertical structure have important impact on the atmospheric thermal radiation. Based on our test results from using the ISCCP's mean-property-based one-layer cloud data, which is an in-house product for diagnostics and produced using ISCCP-H's grid-mean properties, the OLR bias in Table 1 is

reduced to 2.92 W/m^2 from 3.58 W/m^2 and the atmospheric absorption effect is changed to -1.91 W/m^2 from -2.55 W/m^2 , which represent a deduction of more than a half of the differences between the ISCCP and Kuo2017 from the different cloud layer structures alone.

5. Discussion and Conclusions

The cloud scattering effect is ignored or simplified in computation of thermal infrared radiation in most climate studies, because the LW scattering is of secondary importance compared to the absorption effect and the radiative transfer computation is expensive for multiple scattering. In this study, we use the discrete-ordinate algorithm to explicitly consider the LW multiple scattering and evaluate the impact of cloud LW scattering on both the transient and the climatological thermal radiation over the globe.

When cloud LW scattering is considered in radiative transfer, the calculated OLR decreases and both the downward LW flux to the surface and the net atmospheric absorption increase. The LW flux change due to the cloud scattering is concentrated in the infrared atmospheric window spectrum ($800\text{--}1250 \text{ cm}^{-1}$) for low clouds. While for high clouds, the change in downward surface flux is still in the window region but the effect in the OLR is mainly in the far-infrared spectrum ($300\text{--}600 \text{ cm}^{-1}$) because of the low water vapor absorption over high clouds. For clouds with small to moderate optical depth ($\tau < 10$), the scattering effect on thermal fluxes shows large variation with cloud τ . This effect has a maximum around optical depth of 3 and then reaches an asymptote as cloud τ increases. For opaque clouds, the scattering effect is smaller and less important. The scattering effect also increases as cloud particle size decreases because of the enhanced scattering efficiency.

A 2-stream radiative transfer scheme or its equivalent code (e.g., the Delta-Eddington scheme) is commonly used in current climate models. Our simulation indicates that the 2-stream

approximation could have an error over 10% with RMS error around 3.5%-4.0% in the calculated thermal infrared flux when the LW scattering process is considered. This algorithm error of the 2-stream approximation could readily exceed the no-scattering error in LW flux. Therefore, not much can be gained from explicitly including multiple scattering in the LW radiative transfer computation when a 2-stream approximation is used. However, this algorithm error in LW radiation rapidly decreases as stream number increases. The RMS error in LW flux using the 4-stream scheme is under 0.3%. This accuracy is sufficient for climate modeling. Using the analytical solution, the 4-stream scheme is also computationally efficient for radiation computation over long time and global scales. This special 4-stream algorithm is implemented in the radiative transfer code in the GISS climate model (ModelE2.1).

In order to evaluate the impact of neglecting LW scattering on thermal infrared radiation in climate models, we run ModelE with and without the LW scattering effect, respectively. Comparing the thermal fluxes between the two model runs, we find that the global annual mean non-scattering errors in the OLR, the downward surface flux, and the net atmospheric absorption are 2.7 W/m^2 , -1.6 W/m^2 , and -1.8 W/m^2 , respectively. When the LW scattering is neglected, the cooling rate in the troposphere could be increased up to 0.11 K/day. Using one year of ISCCP clouds and running the standalone radiative transfer offline, these global annual mean non-scattering errors are 3.6 W/m^2 , -1.1 W/m^2 , and -2.5 W/m^2 , respectively. The calculated fluxes from ISCCP are transient because no radiation feedback is involved. Considering the great differences in the cloud fields between ISCCP and a climate GCM, the difference in flux bias between ISCCP and the GCM is reasonable and small. When the same cloud optical properties are used, our global mean GCM results are nearly the same as that estimated from one year of satellite observational cloud data by Kuo et al. (2017). The consistency between the

climatological and transient flux changes from neglecting LW scattering may indicate that the cloud feedback has little effect on the no-scattering error in thermal radiation averaged over large spatial scales.

The global scattering impact of 2.7 W/m^2 on the OLR is small when compared to the typical global OLR value of 240 W/m^2 (Kiehl and Trenberth, 1997) and it is right about the current satellite measurement error ($\sim 1\%$) in the OLR (Dewitte and Clerbaux, 2017). However, it is significant when compared to cloud LW radiative forcing (30 W/m^2) and net cloud forcing (-14 W/m^2). The mean scattering effect on global downward flux at the surface of 1.6 W/m^2 is relatively small ($\sim 0.4\%$). Overall, the effect of neglecting LW scattering on the thermal fluxes we estimated here is comparable to the clear sky radiative effect of doubling CO_2 (Clough and Iacono, 1995; Chung and Soden, 2015; Soden et al., 2018) and to the total longwave forcing by the well-mixed greenhouse gases for the period 1860 to 2000 (Collins et al., 2006). It should be noted that the spectral regions affected by the LW cloud scattering have little overlap with the CO_2 absorption bands in the thermal radiation spectrum, and thus, the change in CO_2 concentration in the atmosphere will not change the estimated results much. The decision on whether or not to include the LW scattering depends on the particular application.

Acknowledgement:

Climate modeling at GISS is supported by the NASA Modeling, Analysis, and Prediction program, and resources supporting this work were provided by the NASA High - End Computing Program through the NASA Center for Climate Simulation (NCCS) at Goddard Space Flight Center.

Conflicts of Interest Disclosure

Disclosure: The authors declare no conflicts of interest, financial or non-financial.

Acknowledgement: This study is supported by the NASA Modeling, Analysis, and Prediction program.

References

- Berk, A., G.P. Anderson, P.K. Acharya, and E.P. Shettle, 2008: MODTRAN5 Version 2 USERS MANUAL, SPECTRAL SCIENCES, INC, Burlington MA and Air force Geophysics Laboratory, Hanscom AFB, MA.
- Baum, B. A., Yang, P., Heymsfield, A. J., Bansemer, A., Cole, B. H., Merrelli, A., . . . Wang, C. (2014). Ice cloud single-scattering property models with the full phase matrix at wavelengths from 0.2 to 100 mm. *Journal of Quantitative Spectroscopy and Radiative Transfer*, 146, 123–139. <https://doi.org/10.1016/j.jqsrt.2014.02.029>
- Cess, R. D., et al. (1990). Intercomparison and Interpretation of Climate Feedback Processes in 19 Atmospheric General Circulation Models. *J. Geophys. Res.* 95 (D10): 16, 601–16, 615. Bibcode:1990JGR....9516601C. doi:10.1029/jd095id10p16601.
- Chandrasekhar, S. (1960). *Radiative Transfer*. Dover Publications Inc., p. 393. ISBN 978-0-486-60590-6.
- Chou, M.-D., 1999: Parameterization for cloud longwave scattering for use in atmospheric models. *J. Climate*, 12, 159-169.
- Chung, E.-S. and Soden, B. J., 2015: An assessment of methods for computing radiative forcing in climate models, *Environ. Res. Lett.*, 10, 074004, <https://doi.org/10.1088/1748-9326/10/7/074004>.

- Clough, S. A., & Iacono, M. J. (1995). Line-by-line calculation of atmospheric fluxes and cooling rates: 2. Application to carbon dioxide, ozone, methane, nitrous oxide and the halocarbons. *J. Geophys. Res.*, 100(D8), 16519–16535. doi:10.1029/95JD01386
- Collins W. D. et al. (2006). Radiative forcing by well-mixed greenhouse gases: estimates from climate models in the intergovernmental panel on climate change (IPCC) fourth assessment report (AR4) *J. Geophys. Res.*, 111, D14317.
- Costa, S. M. S., & Shine, K. P. (2006). An estimate of the global impact of multiple scattering by clouds on outgoing long-wave radiation. *Quarterly Journal of the Royal Meteorological Society*, 132(616), 885–895. <https://doi.org/10.1256/qj.05.169>
- Dewitte, S. and N. Clerbaux, 2017: Measurement of the Earth radiation budget at the top of the atmosphere - A review. *Remote Sens.*, 9, 1143; doi:10.3390/rs9111143.
- Fu, Q., K. N. Liou, M. C. Cribb, T. P. Charlock, and A. Grossman, 1997: Multiple scattering parameterization in thermal infrared radiative transfer. *J. Atmos. Sci.*, 54, 2799–2812, [https://doi.org/10.1175/1520-0469\(1997\)054,2799:MSPITI.2.0.CO;2](https://doi.org/10.1175/1520-0469(1997)054,2799:MSPITI.2.0.CO;2).
- Han, Q., W. B. Rossow, and A. A. Lacis (1994), Near-global survey of effective droplet radii in liquid water clouds using ISCCP data, *J. Clim.*, 7, 465– 497.
- Han, Q., W. B. Rossow, J. Chou, K.-S. Kuo, and R. M. Welch (1999), The effects of aspect ratio and surface roughness on satellite retrievals of ice cloud properties, *J. Quant. Spectrosc. Radiat. Trans.*, 63, 559–583.
- Hu, Y. X., and K. Stamnes, 1993: An accurate parameterization of the radiative properties of water clouds suitable for use in climate models. *J. Climate*, 6, 728–742, [https://doi.org/10.1175/1520-0442\(1993\)006,0728:AAPOTR.2.0.CO;2](https://doi.org/10.1175/1520-0442(1993)006,0728:AAPOTR.2.0.CO;2).

- Jin, Z., T.P. Charlock, K. Rutledge, K. Stamnes, and Y. Wang, 2006: Analytical solution of radiative transfer in the coupled atmosphere-ocean system with a rough surface. *Appl. Opt.*, 45, 7443-7455.
- Justice, C. O., et al., 1998: The Moderate Resolution Imaging Spectroradiometer (MODIS): Land remote sensing for global change research, *IEEE Trans. Geosci. Remote Sens.*, 36, 1228–1249, doi:10.1109/36.701075.
- King, M. D., S. Platnick, W. P. Menzel, S. A. Ackerman, and P. A. Hubanks, (2013), Spatial and Temporal Distribution of Clouds Observed by MODIS Onboard the Terra and Aqua Satellites, *IEEE Trans. Geosci. Remote Sensing*, V. 51, NO. 7, July 2013.
- Kuo, C.-P., P. Yang, X. Huang, D. Feldman, M. Flanner, C. Kuo, and E. Mlawer, 2017: Impact of multiple scattering on LW radiative transfer involving clouds. *J. Adv. Model. Earth Syst.*, 9, 3082–3098.
- Lacis, A. A., and V. Oinas, 1991: A description of the correlated k distribution method for modeling nongray gaseous absorption, thermal emission and multiple scattering in vertically inhomogeneous atmospheres. *J. Geophys. Res.*, 96, 9027–9063.
- Li, J., 2002: Accounting for unresolved clouds in a 1d infrared radiative transfer model. Part I: Solution for radiative transfer, including cloud scattering and overlap. *J. Atmos. Sci.*, 59, 3302–3320.
- Li, J. and Q. Fu, 2000: Absorption approximation with scattering effect for infrared radiation. *J. Atmos. Sci.*, 57, 2905–2914.
- Liou, K. N., 2002: *An Introduction to Atmospheric Radiation*. Second Edition. Academic Press.

- Kiehl, J.T., and K.E. Trenberth, 1997: Earth's Annual Global Mean Energy Budget. *Bull. Amer. Meteorol. Soc.*, 78, 197-208.
- Mace, G.G., and Q. Zhang, 2014: The CloudSat radar-lidar geometrical profile product (RL-GeoProf): Updates, improvements, and selected results. *J. Geophys. Res. Atmos.*, 119, 9441-9462.
- W.E. Meador and W.R. Weaver, 1980, Two-Stream Approximations to Radiative Transfer in Planetary Atmospheres: A Unified Description of Existing Methods and a New Improvement, 37, *J. Atmos. Sci.*, 630-643.
<http://journals.ametsoc.org/doi/pdf/10.1175>
- Oinas, V., A. A. Lacis, D. Rind, D. T. Shindell, and J. E. Hansen, 2001: Radiative cooling by stratospheric water vapor: Big differences in GCM results. *Geophys. Res. Lett.*, 28, 2791-2794.
- Platnick, S., and Coauthors, 2017: The MODIS cloud optical and microphysical products: Collection 6 updates and examples from Terra and Aqua. *IEEE Trans. Geosci. Remote Sens.*, 55, 502-525, <https://doi.org/10.1109/TGRS.2016.2610522>
- Rossow, W. B., and R. A. Schiffer (1999), Advances in understanding clouds from ISCCP, *Bull. Am. Meteorol. Soc.*, 80, 2261- 2287.
- Rossow, W.B., and Y.-C. Zhang, 2010: Evaluation of a statistical model of cloud vertical structure using combined CloudSat and CALIPSO cloud layer profiles. *J. Climate*, 23, 6641-6653, doi:10.1175/2010JCLI3734.1
- Schmidt, G. A., Ruedy, R., Hansen, J. E., Aleinov, I., Bell, N., Bauer, M., . . . Yao, M.-S. (2006). Present-day atmospheric simulations using GISS ModelE: Comparison to in situ, satellite, and reanalysis data. *Journal of Climate*, 19(2), 153-192.

- Schmidt, G.A., and Coauthors, 2014: Configuration and assessment of the GISS ModelE2 contributions to the CMIP5 archive. *J. Adv. Model. Earth Syst.*, 6, no. 1, 141-184.
- BJ Soden, WD Collins, DR Feldman, 2018: Reducing uncertainties in climate models. *Science*, 361 (6400), 326-327, doi: 10.1126/science.aau1864.
- Stamnes, K., Tsay, S.-C., Wiscombe, W., & Jayaweera, K. (1988). Numerically stable algorithm for discrete-ordinate-method radiative transfer in multiple scattering and emitting layered media. *Applied Optics*, 27(12), 2502–2509.
- Stephens, G. L., P. M. Gabriel, and P. T. Partain, 2001: Parameterization of atmospheric radiative transfer. Part I: Validity of simple models. *J. Atmos. Sci.*, 58, 3391–3409.
- Tang, G., P. Yang, G. W. Kattawar, X. Huang, E. J. Mlawer, B. A. Baum, and M. D. King, 2018: Improvement of the simulation of cloud longwave scattering in broadband radiative transfer models. *J. Atmos. Sc.*, 75, 2217-2233.
- Wu, K., J. Li, J. Cole, X. Huang, K. v. Salzen, and F. Zhang, 2019: Accounting for Several Infrared Radiation Processes in Climate Models, *J. Climate*, 32, 15, <https://doi.org/10.1175/JCLI-D-18-0648.1>
- Young, A. H., Knapp, K. R., Inamdar, A., Hankins, W., and Rossow, W. B.: The International Satellite Cloud Climatology Project H-Series climate data record product, *Earth Syst. Sci. Data*, 10, 583-593, <https://doi.org/10.5194/essd-10-583-2018>, 2018.
- Zhang, Y.C., Rossow, W.B, Andrew A. Lacis, A.A and Oinas, V. (2019): Calculation, evaluation and application of long-term, global radiative flux Datasets at ISCCP: Past and present. Submitted for “Study of Cloud and Water Processes in Weather and Climate through Satellite Observations”, the book, to be published by World Scientific Publishing Company as the second volume in a multi-part series on Earth sciences. (Also see

<https://isccp.giss.nasa.gov/projects/flux.html> ☐ <https://isccp.giss.nasa.gov/pub/flux-fh/docs/> for ISCCP-FH product information).

Zhang, Y.-C., W.B. Rossow, A.A. Lacis, V. Oinas, and M.I. Mishchenko, 2004: Calculation of radiative fluxes from the surface to top of atmosphere based on ISCCP and other global data sets: Refinements of the radiative transfer model and the input data. *J. Geophys. Res.*, 109, D19105, doi:10.1029/2003JD004457.

Zhao, W., Y. Peng, B. Wang, and J. Li, 2018: Cloud longwave scattering effect and its impact on climate simulation. *Atmosphere*, 9, 153, <https://doi.org/10.3390/atmos9040153>.

Table 1. Global Mean LW Radiation Biases (W/m^2) From Neglecting LW Scattering

Model	Upward Flux (TOA)	Downward Flux (Surface)	Atmospheric Absorption
<i>GCM(Aggregate Ice)</i>	2.67	-1.58	-1.74
<i>GCM(Solid Column Ice)</i>	2.74	-1.56	-1.80
<i>ISCCP(Aggregate Ice)</i>	3.58	-1.08	-2.55
<i>Kuo2017(Aggregate Ice)</i>	2.6	-1.2	-1.4

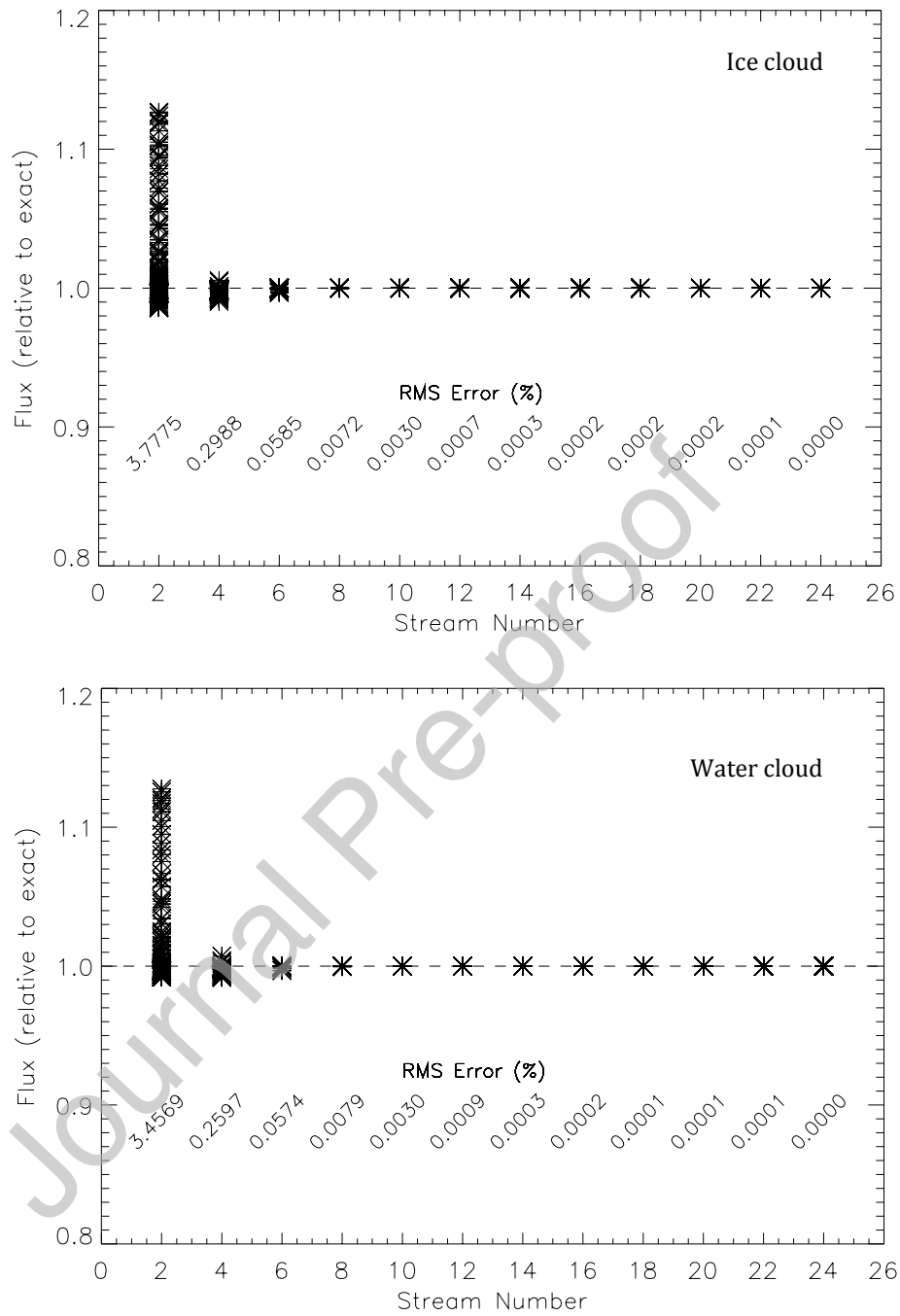


Fig. 1. LW fluxes calculated by different stream numbers. A single layer cloud is assumed (see text). There are 200 cloud cases under each stream number and the fluxes are normalized by the benchmark value. A divergence from the 1.0 in the normalized flux represents the computation error. The RMS error in % for each stream is shown under the flux plot.

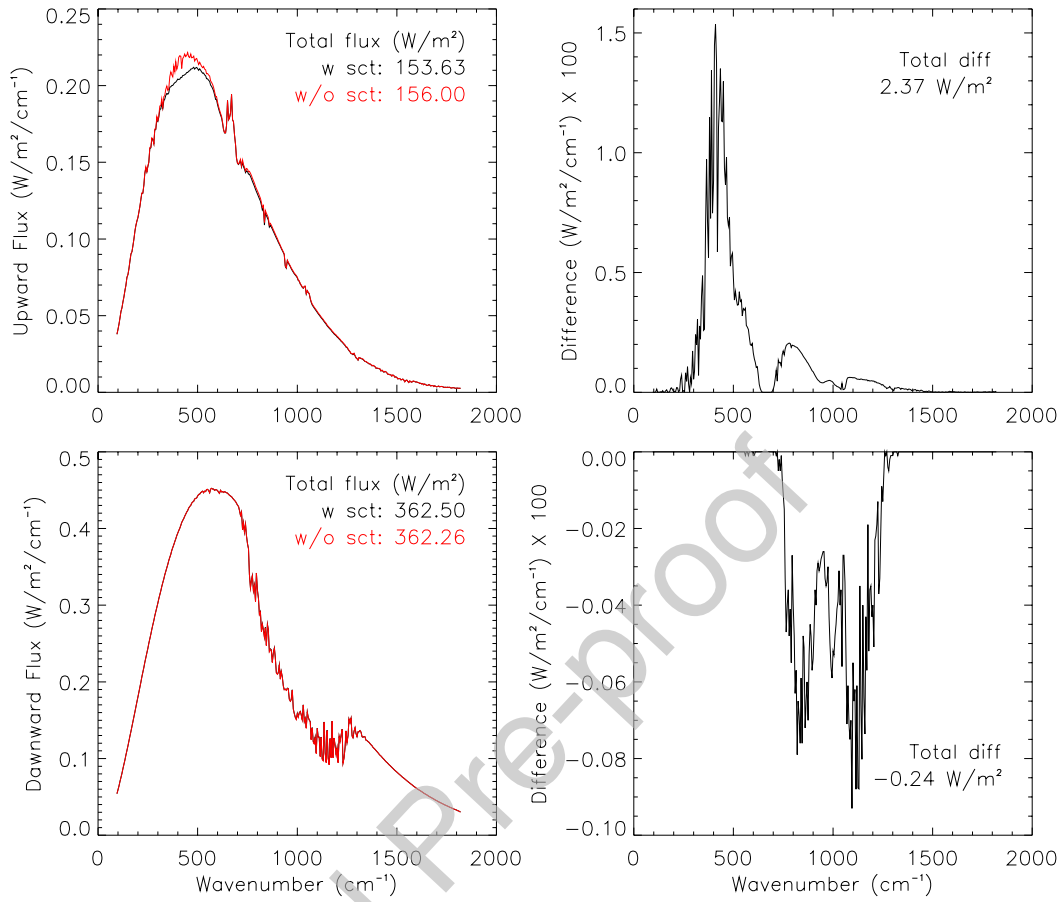


Fig. 2a. Left: comparison of the spectral LW fluxes calculated with (black) and without (red) cloud scattering effect. Right: the difference between the two (without scattering – with scattering) for a high cloud (ice, $\tau=10$, $R_e=40 \mu\text{m}$, top height at 11 km).

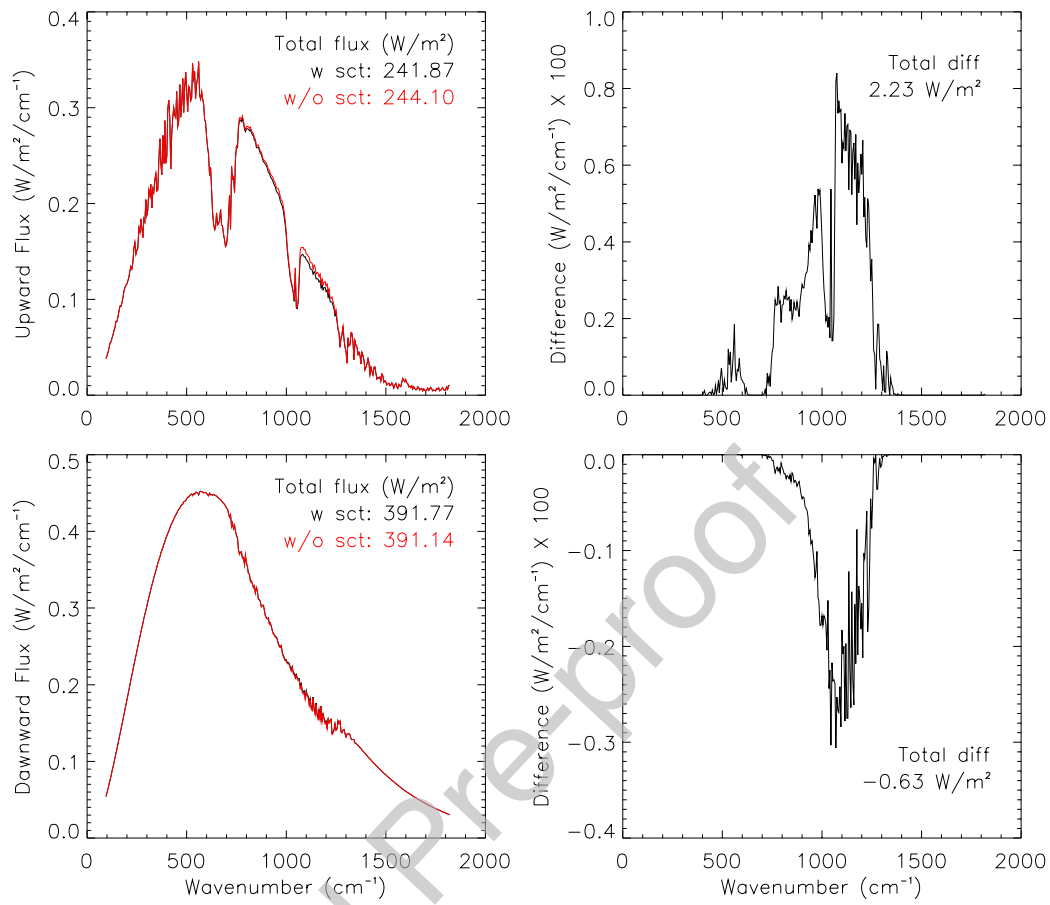


Fig. 2b. Same as (1a) except for a low cloud (water, $\tau=10$, $R_e=10 \mu\text{m}$, top height at 4 km).

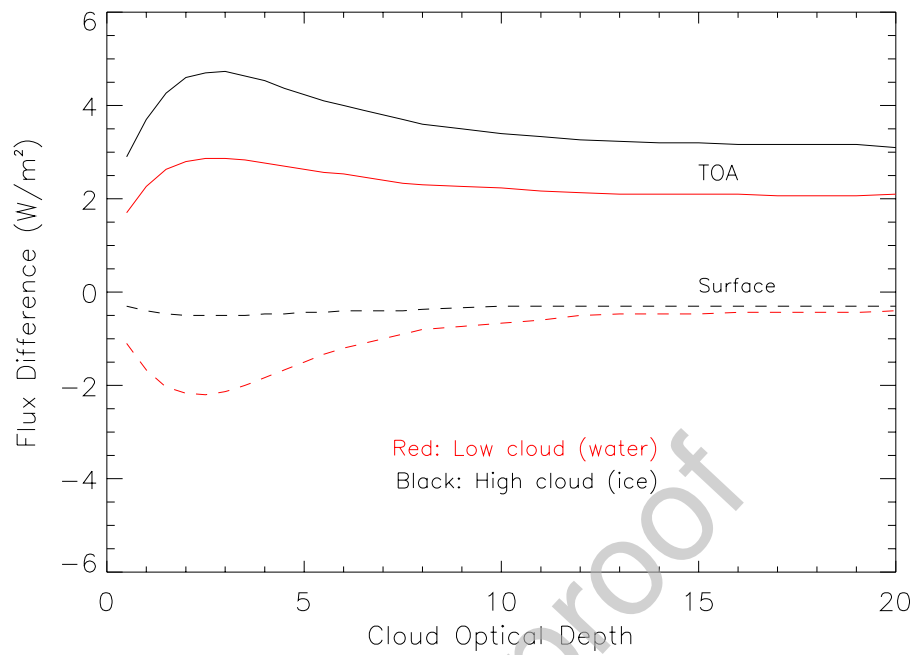


Fig. 3. The no-scattering thermal radiation error as a function of cloud optical depth for the high (black) and low (red) clouds defined in Figure 1. Solid lines represent the OLR and the dashed lines represent the downward LW flux at the surface.

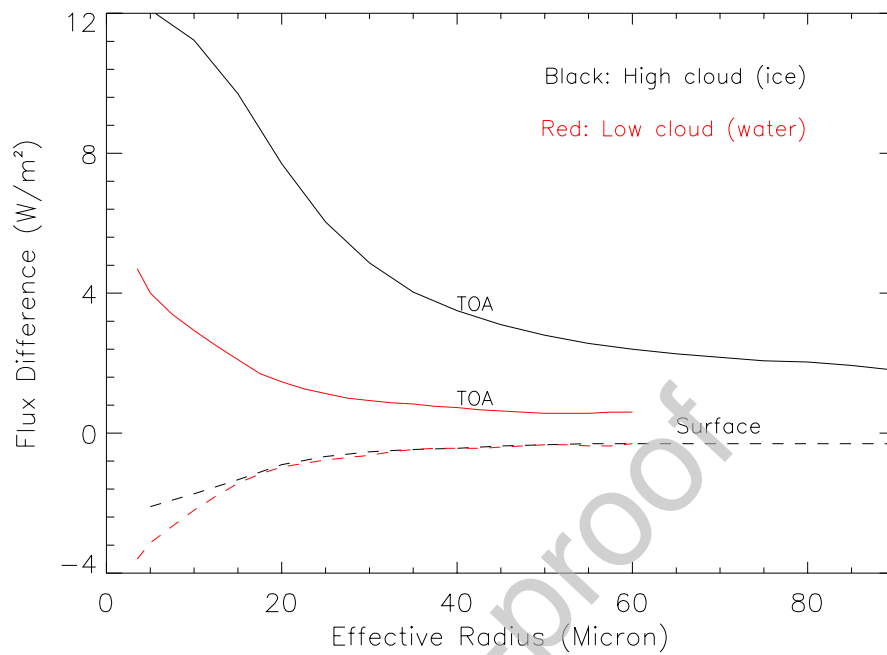


Fig. 4. The no-scattering thermal radiation error as a function of cloud particle size for the high (black) and low (red) clouds with physical properties defined in Figure 1 ($\tau=3$). Solid lines represent the OLR and the dashed lines represent the downward LW flux at the surface.

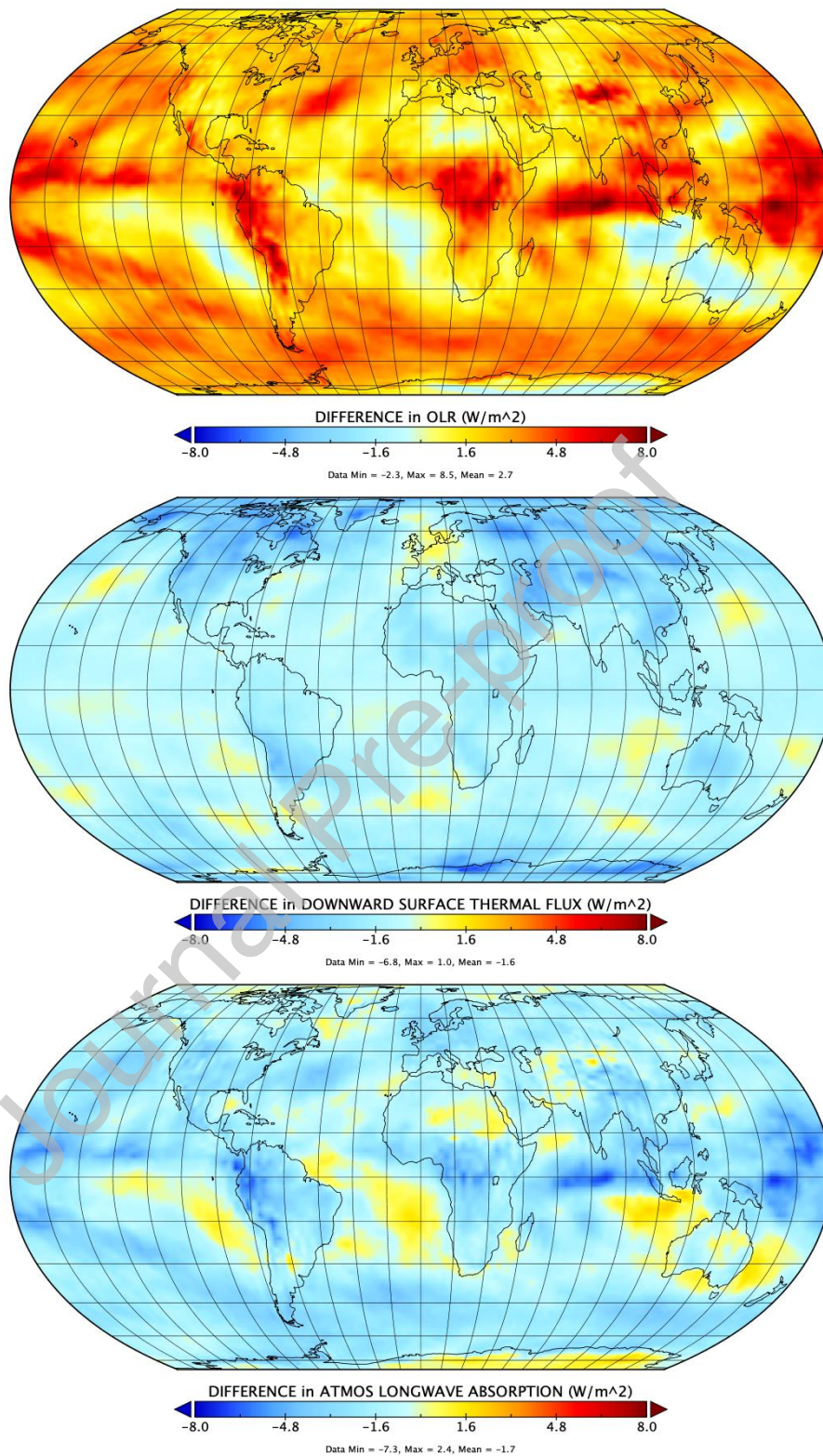


Fig. 5. Annual mean biases due to neglecting the LW scattering for (a) the OLR, (b) the downward flux at the surface, and (c) the net atmospheric absorption. Results are averaged from 20-yr GCM simulation.

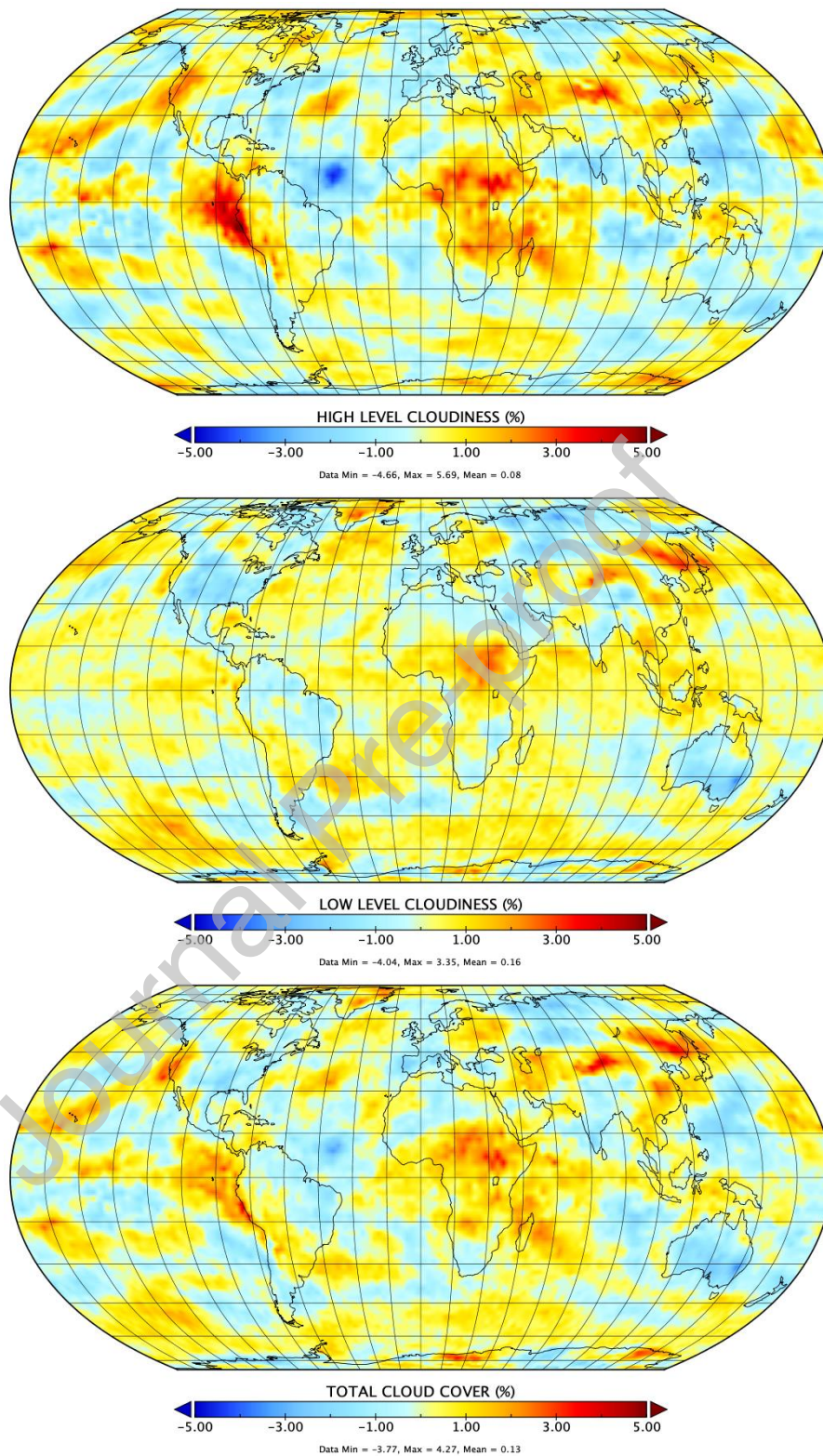


Fig 6. 20-yr average change of cloudiness due to neglecting the LW scattering.

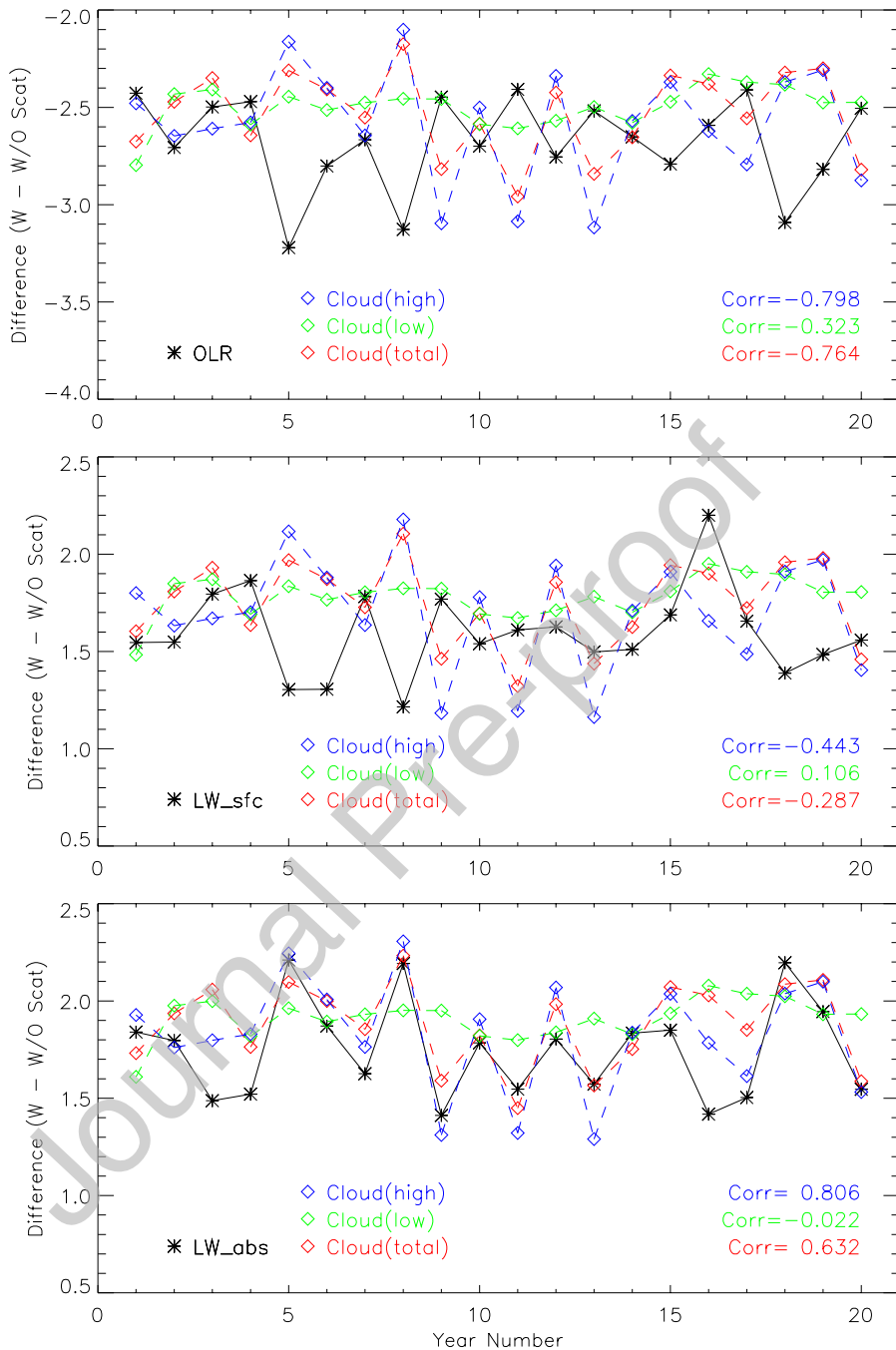


Fig 7. The global annual means of the scattering effect on the LW radiation (W/m^2) and cloudiness (%). The black lines in the upper, middle, and lower panels represent the OLR, the downward surface flux and the atmospheric absorption, respectively. The three colored lines represent the changes in high, low and total cloudiness (%), respectively, and the cloudiness changes in each panel are offset by the 20-year mean of radiation change. The numbers in the lower right corner represent the correlation coefficients of the changes in radiation and cloud amount.

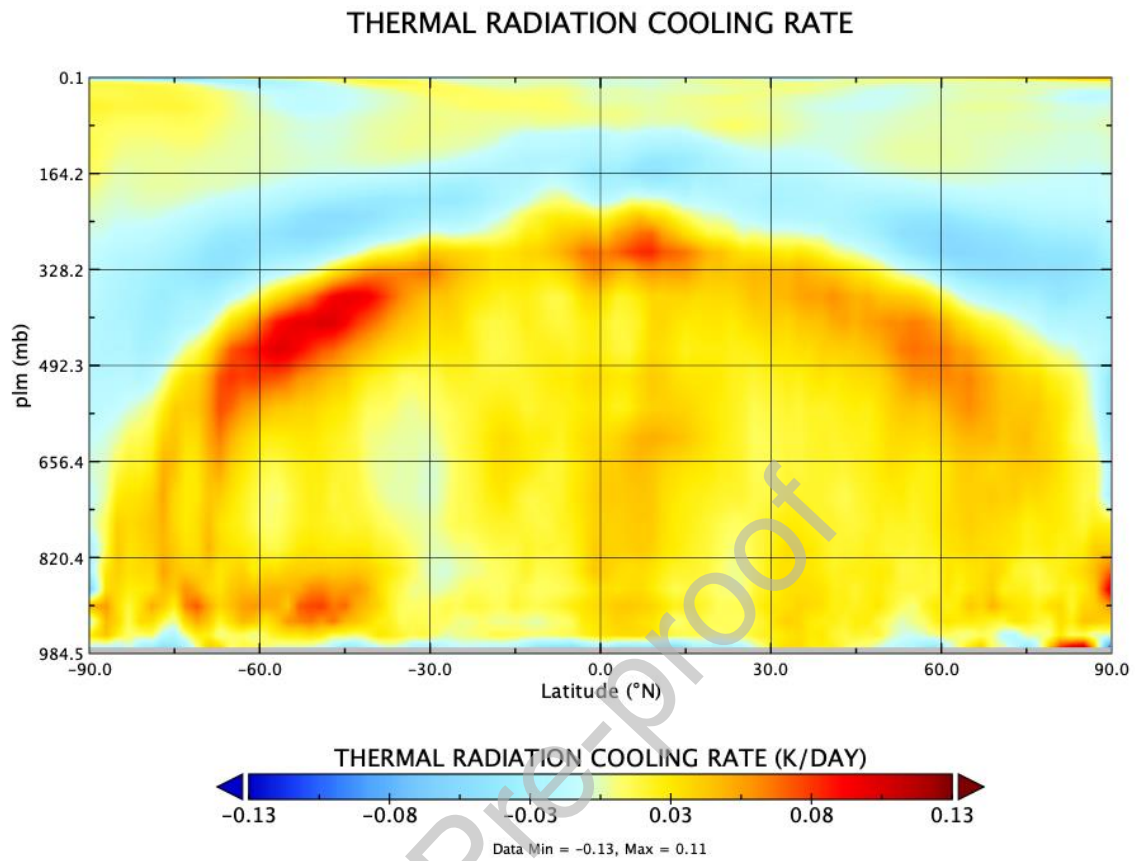


Fig 8. The 20-yr average change of cooling rate due to neglecting the LW scattering.

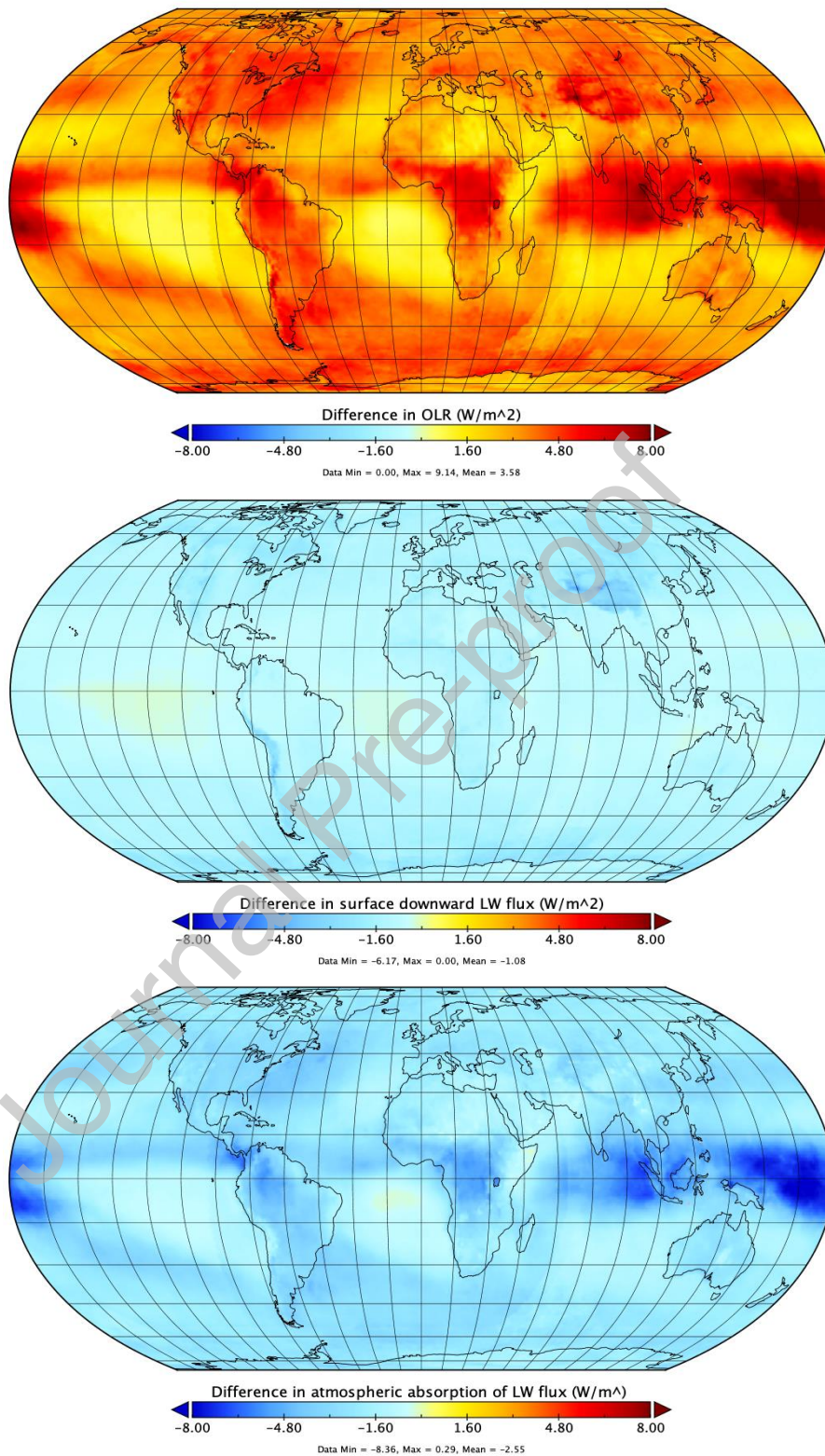


Fig. 9. Same as Figure 5 but based on 1993 ISCCP-H data.

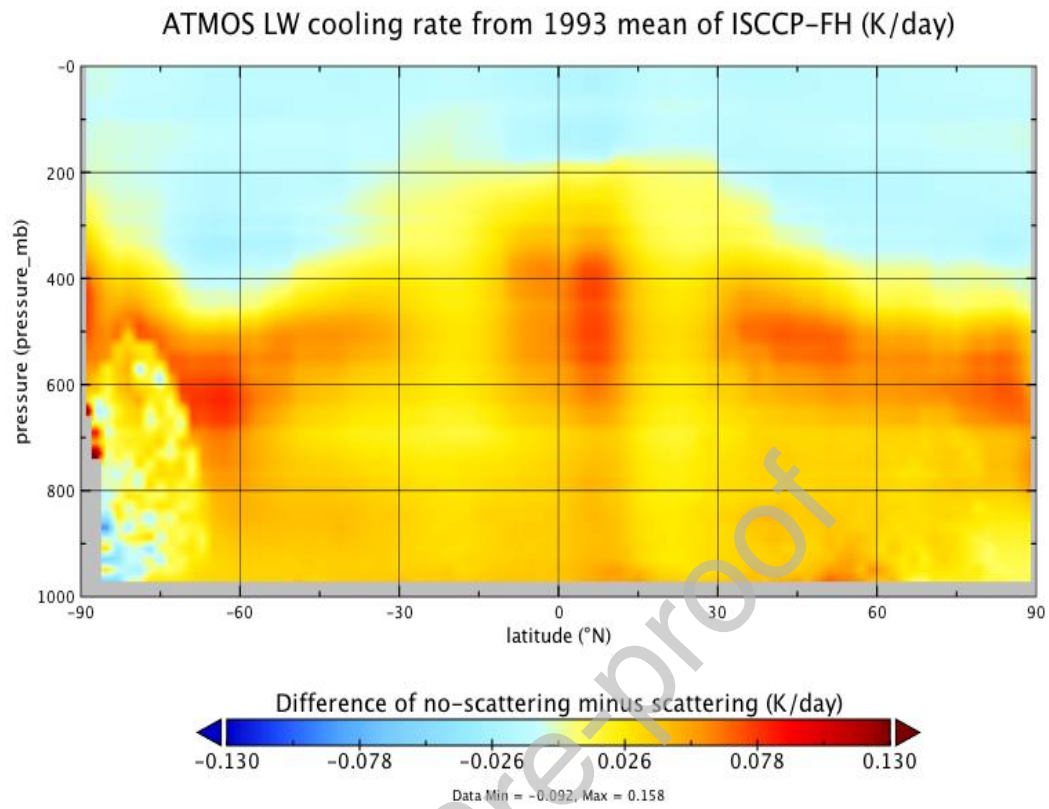


Fig. 10. Same as Figure 7 but calculated based on the 1993 ISCCP-H data.

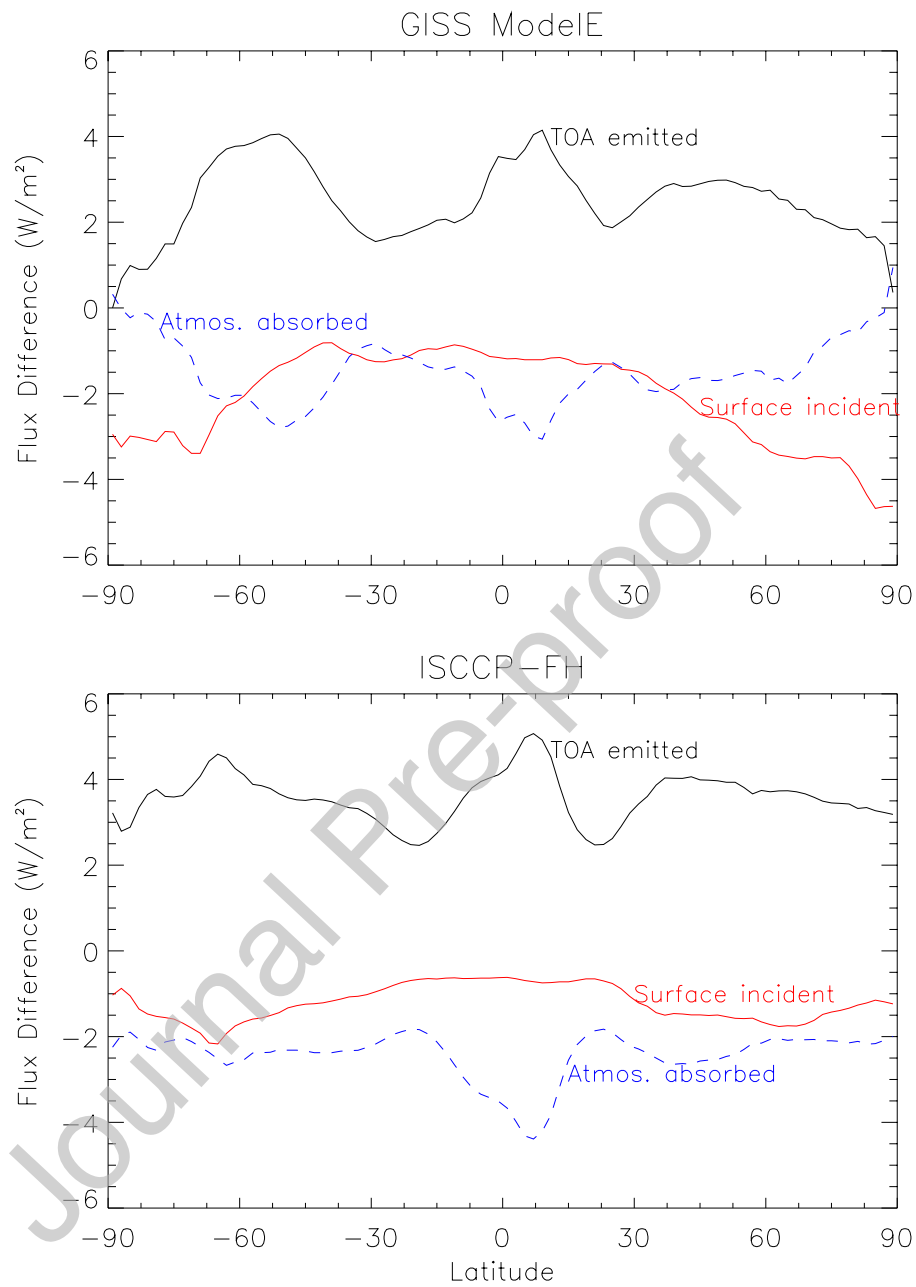


Fig. 11. Zonal average thermal radiation errors from neglecting LW cloud scattering. The black, red and blue lines represent the flux biases in the OLR at TOA, the downward flux at the surface and the atmospheric absorption, respectively.